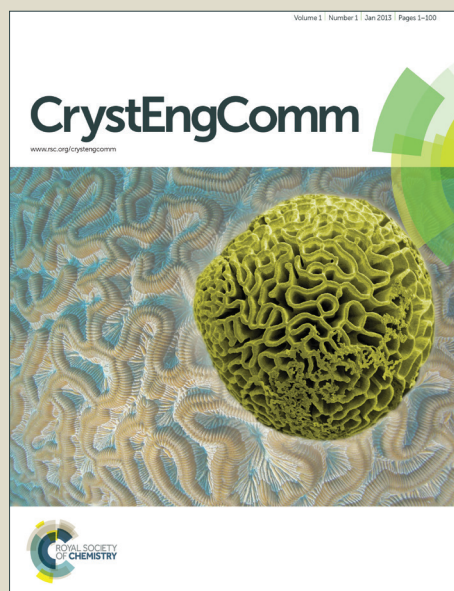


CrystEngComm

Accepted Manuscript



This is an *Accepted Manuscript*, which has been through the Royal Society of Chemistry peer review process and has been accepted for publication.

Accepted Manuscripts are published online shortly after acceptance, before technical editing, formatting and proof reading. Using this free service, authors can make their results available to the community, in citable form, before we publish the edited article. We will replace this *Accepted Manuscript* with the edited and formatted *Advance Article* as soon as it is available.

You can find more information about *Accepted Manuscripts* in the [Information for Authors](#).

Please note that technical editing may introduce minor changes to the text and/or graphics, which may alter content. The journal's standard [Terms & Conditions](#) and the [Ethical guidelines](#) still apply. In no event shall the Royal Society of Chemistry be held responsible for any errors or omissions in this *Accepted Manuscript* or any consequences arising from the use of any information it contains.

Cite this: DOI: 10.1039/cxxxxxxx

www.rsc.org/crystengcomm

COMMUNICATION

Enhanced water stability of a microporous acylamide-functionalized Metal-Organic Framework via interpenetration and methyl decoration†

Baishu Zheng,^{*a} Xiu Lin^a, Zhaoxu Wang,^{*a} Ruirui Yun^b, Yanpeng Fan^a, Mingsheng Ding^a, Xiaolian Hu^a and Pinggui Yi^{*a}

⁵ Received (in XXXX, XXX) Xth XXXXXXXXXX 201X, Accepted Xth XXXXXXXXXX 201X
DOI: 10.1039/c000000000x

A microporous acylamide-functionalized MOF with 2-fold interpenetrated and methyl decorated framework (HNUST-4) has been designed and synthesized from [Cu₂(COO)₄] motifs and a C₂-symmetric acylamide-linking tetracarboxylate, which exhibits good water stability, permanent porosity, high and selective CO₂ uptake at ambient temperature.

Metal-organic frameworks (MOFs) have become a leading class of porous crystalline materials for potential applications in gas storage¹, gas separation² and catalysis³. These applications mainly hinge on two important properties of MOFs: porosity and stability. Currently, remarkable breakthroughs in the construction of MOFs with ultrahigh porosity have been reported and several landmark MOFs display large experimental BET surface area with values exceeding 5000 m²/g.⁴ However, most of such highly porous MOFs are not robust enough and prone to collapse at humid environments, which greatly hinders their practical gas storage/separation applications. Thus, how to design and address porous materials with high hydrostability is one of the key challenges we now face in MOF chemistry, and several strategies are envisaged to achieve this goal: (i) strengthening the metal-ligand coordination bonds by judicious choice of metal ions/clusters and organic ligands (e.g. high oxidation state metals such as Fe³⁺, Cr³⁺, Al³⁺ and Zr⁴⁺, etc for carboxylate-based MOFs⁵ and nitrogen-containing linkers such as pyrazole, imidazole and pyridyl-carboxylate, etc for transition-metal based MOFs or ZIFs⁶); (ii) utilizing interpenetration or catenation⁷ to narrow the pore size; (iii) doping hybrid composites (e.g. carbon nanotubes, hetero-metal) to the frameworks⁸ and (iv) decorating the pores by

hydrophobic groups (e.g. methyl, ethyl ester, etc).⁹

In pursuing new high-performance gas storage/separation materials, we are specially interested in the design and construction of porous MOFs from large multidentate carboxylate ligands with linking polar functional groups (e.g. acylamide, oxalamide, etc.) and dicopper(II) paddlewheel cluster, because such an approach may facilitate the generation of expanded MOFs with high surface area, open copper sites and pre-designed polar functionalities that are all beneficial to improve the gas (especially for CO₂) adsorption and separation property of materials.¹⁰ To extend our research in this area, herein we report a novel 2-interpenetrated microporous acylamide-functionalized MOF decorated by methyl groups, termed HNUST-4 (HNUST denotes Hunan University of Science and Technology), designed from a nanosized flexible tetracarboxylate 5,5'-[(5-methyl-1,3-phenylene)bis(carbonylimino)]diisophthalic acid (MPBD). Interestingly, HNUST-4 represents a rare example of water-stable MOFs constructed from paddlewheel SBUs and pure carboxylate ligands, its crystallinity can be sustained even after immersion in boiling water for a day. In addition, HNUST-4 exhibits a moderate BET surface area of 1136 m²·g⁻¹, high and selective CO₂ uptake at ambient temperature.

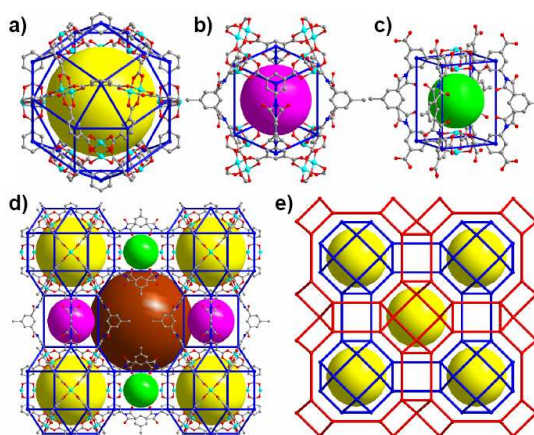


Fig. 1 The crystal structure of HNUST-4. a-c) different cages in the crystal structure; d-e) single and 2-interpenetrated network viewed from *b* and *c* axis, respectively. Cu, blue-green; C, black; O, red; N, blue. Water molecules and H atoms have been omitted for clarity.

^a Key Laboratory of Theoretical Organic Chemistry and Function Molecule of Ministry of Education, School of Chemistry and Chemical Engineering, Hunan University of Science and Technology, Xiangtan 411201, China. E-mail: zbaishu@163.com; hnuist_chem@163.com; yipinggui@sohu.com.

^b College of Chemistry and Materials Science, Anhui Normal University, Wuhu 241000, China.

† Electronic supplementary information (ESI) available: Experimental details, TGA plots, heat adsorption of H₂, CO₂ and CH₄, sorption selectivity calculations. CCDC 1006012. For ESI and crystallographic data in CIF or other electronic format see DOI: 10.1039/b000000x/

Solvothermal reaction of MPBD and $\text{Cu}(\text{NO}_3)_2 \cdot 3\text{H}_2\text{O}$ in DMF/ethanol/ H_2O (5:3:2 in volume) at 75 °C for 48 hours afforded pale blue block crystals of HNUST-4. HNUST-4 crystallizes in space group $I4/mmm$ and the framework consists of $[\text{Cu}_2(\text{COO})_4]$ paddlewheels linked by MPBD⁺ ligands. MPBD⁺ exhibits two crystallographically independent conformations (*syn*- and *anti*-) and the carbonyl moiety of acylamide group is disordered over two positions with equal probability (Fig. S1). Similar to the isostructural PMOF-3 and analogues¹¹, the overall structure of HNUST-4 exhibits 2-fold interpenetration and each single framework can be viewed as the packing of three types of cages in 3D space (Fig. 1a-c): Cage A is a cuboctahedron composed of twenty-four isophthalate units and twelve paddlewheels with a diameter of 1.2 nm. Cage B, a tetragonal prismatic junction-like cage about 1.3 nm in diameter, is formed from four paddlewheels and four *anti*-MPBD⁺ linkers. Cage C is also a tetragonal prismatic junction-like cage of about 0.8 nm diameter, surrounded by four *syn*-MPBD⁺ and two paddlewheels. Each cage A is connected to six neighboring cages A via two cages B and four cages C to form a 3D framework with a simple cubic network topology, in which there exists large 1D rounded-like channel along the *c* axis with a diameter of about 3.0 nm (Fig. S1). Notably, this channel is further filled by cage A from the other interpenetrating framework due to the large void space, despite that the channel has been occupied by methyl groups, resulting in a 2-fold interpenetrated structure (Fig. 1e) of HNUST-4 with a total potential solvent accessible volume of about 53.6 % upon removal of guest molecules calculated by PLATON¹².

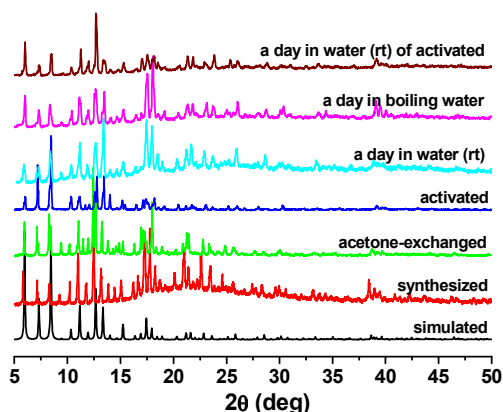


Fig. 2 Powder X-ray diffraction patterns of HNUST-4, showing the framework stability upon treatment at different conditions.

To assess the framework stability of HNUST-4, both the thermogravimetric analysis (TGA) and powder X-ray diffraction (PXRD) measurements have been performed. The TGA curve indicates that HNUST-4 can be thermally stable up to 300 °C (Fig. S3). In addition, as shown in Fig. 2, the PXRD patterns of HNUST-4 demonstrate that the single crystal is representative of the pure bulk sample, and the framework can be retained after removal of guest molecules. Most interestingly, HNUST-4 exhibits good water stability and

the as-synthesized sample can sustain its crystallinity even when immersed in boiling water for a day. Furthermore, the desolvated HNUST-4, which can be obtained by heating the acetone-exchanged sample under high vacuum at 100 °C for 12 h, also demonstrates framework stability after treatment in water at room temperature. To the best of our knowledge, HNUST-4 thus represents the second example of water stable acylamide-functionalized MOFs constructed from paddlewheel SBUs and pure carboxylate ligands. Another instance, PCN-124 with a self-interpenetrated (3, 36)-connected 3D structure recently reported by Zhou group^{7b}, also shows moderate water stability at room temperature. The excellent hydrostability of HNUST-4 may be attributed to the interpenetrated framework and incorporated hydrophobic methyl groups, both factors are believed to can effectively enhance the hydrostability of MOFs.^{7,9}

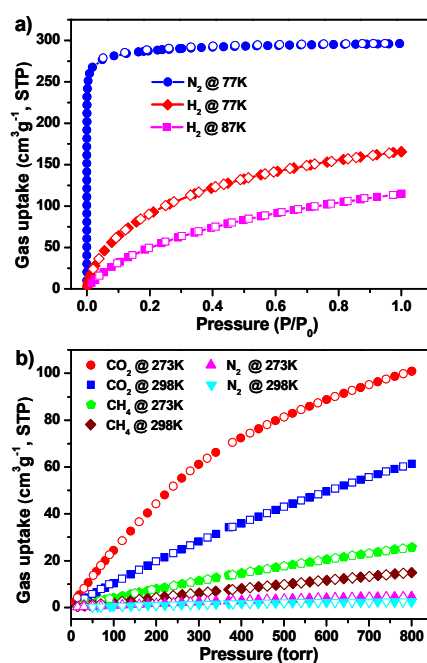


Fig. 3 Gas sorption isotherms of HNUST-4 up to 1 bar at different temperatures.

The permanent porosity of desolvated HNUST-4 was examined via low-pressure N₂ adsorption measurements at 77 K. HNUST-4 shows completely reversible type-I adsorption behavior, characteristic of microporous materials with the high limiting N₂ uptakes of 296 cm³ g⁻¹ (Fig. 3a). The estimated apparent Brunauer–Emmett–Teller (BET) surface area is 1136 m² g⁻¹ (Langmuir surface area ~ 1284 m² g⁻¹) and the total pore volume is 0.458 cm³ g⁻¹, which is comparable to the theoretically total framework pore volume (0.536 cm³ g⁻¹) calculated by PLATON. In addition, HNUST-4 possesses a pore-size distribution with the pore sizes centered at 8.6, 9.3 and 11.8 Å, respectively (Fig. S5), consistent with the single crystal data.

The permanent porosity, open copper sites and acylamide functional groups within the hydrostable framework of HNUST-4 prompted us to study its gas adsorption performance, especially that for CO₂ capture and separation (CCS). Thus, low-pressure H₂,

CO₂, CH₄ and N₂ sorption isotherms of HNUST-4 at different temperatures have been measured (Fig. 3). All isotherms are fully reversible and HNUST-4 can adsorb 1.52 and 1.02 wt% (170.3 and 114.6 cm³ g⁻¹) at 77 and 87 K (1 bar) without saturation, respectively, which is quite close to the performance of MOFs PCN-6' (1.37 wt %) ^{13a} and HKUST-1 (1.44 wt %) ^{13b} at 77 K and 1 bar. Based on the adsorption isotherms measured at 77 K and 87 K, the zero coverage H₂ adsorption enthalpy (Q_{st}) of HNUST-4 is calculated to be 7.0 kJ mol⁻¹ by the virial method (Fig. S6), comparable with those of MOFs with exposed metal sites. ¹⁴ Noticeably, HNUST-4 exhibits high CO₂ uptakes of 100.9 and 62.9 cm³ g⁻¹ under 1 bar at 273 and 298 K, respectively. This CO₂ storage capacity is lower than those of other acylamide-functionalized MOFs such as HNUST-1 ^{10c} (156.4 cm³ g⁻¹ at 273 K and 1 bar), HNUST-3 ^{10d} (168.7 cm³ g⁻¹ at 273 K and 1 bar) and PCN-124 ^{7b} (204 cm³ g⁻¹ at 273 K and 1 bar) owing to the relatively low BET surface area, but fairly comparable to that of SUN-50 ^{15a} (106 cm³ g⁻¹ at 273 K and 1 bar) and PCN-124 analogue Cu₂L ^{15b} [63.5 cm³ g⁻¹ at 298 K and 1 bar, L = 3,5-bis(3,5-dicarboxylphenylethynyl) pyridine], and quite larger than that of the best performing ZIF material ZIF-20 ^{15c-d} (69.8 cm³ g⁻¹ at 273 K and 1 bar). In sharp contrast to CO₂, HNUST-4 can only uptake limited amounts of CH₄ (24.7 and 14.3 cm³ g⁻¹) and N₂ (4.4 and 2.5 m³ g⁻¹) under 1 bar at 273 and 298 K, indicating that HNUST-4 has the ability to selectively adsorb CO₂ over CH₄ and N₂. The CO₂/CH₄ and CO₂/N₂ adsorption selectivities calculated from the slopes of the isotherms reach up to 6.3 and 29.9 at 273 K, respectively (the values still reach 4.9 and 20.6 at 298 K, Fig. S7), much higher than the corresponding values of most MOFs with high surface area (mainly in the ranges of 3–10 and 10–50 for CO₂/CH₄ and CO₂/N₂ selectivity at 298 K). ¹⁶

To better understand these observations, the coverage-dependent Q_{st} of HNUST-4 to CO₂ and CH₄ were also calculated by the virial method, from fits of the adsorption isotherms collected at 273 and 298 K. As shown in Fig. S6, the Q_{st} of CO₂ is 27.2 kJ mol⁻¹ at the zero coverage, which compares well with the reported data for other acylamide-functionalized MOFs such as [Cu₂₄(TPBMTM⁶)₈] (26.3 kJ mol⁻¹) ^{9a}, indicating a strong interaction between CO₂ and HNUST-4. As for CH₄, HNUST-4 exhibits a lower Q_{st} value (18.5 kJ mol⁻¹) at zero coverage. The excellent CO₂ adsorption behaviour of HNUST-4 may be attributed to the large dipole moment of the -CONH- groups, which may facilitate strong dipole-quadrupole interactions between the acylamide groups within HNUST-4 and CO₂.

In summary, by utilizing a nanosized acylamide-bridging tetracarboxylate (MPBD) as the linker and a copper(II) paddlewheel as the SBU, we have successfully designed and constructed a new microporous acylamide-functionalized MOF (HNUST-4). HNUST-4 possesses 2-fold interpenetrated structure with decorated methyl groups, exhibiting good water-stability, a moderate BET surface area of 1136 m² g⁻¹, high CO₂ uptake capacity (100.9 and 62.9 cm³ g⁻¹ under 1 bar at 273 and 298 K), as well as excellent CO₂/CH₄ and CO₂/N₂ selectivity at ambient temperature. This work demonstrates that the strategy of interpenetration together with hydrophobic methyl decoration is an effective method to enhance the

hydrostability of MOF materials. Ongoing investigations are addressing such water stable acylamide-functionalized MOFs with even higher surface area and pore volume by using larger linkers or highly connected SBUs to further improve the CO₂ uptake and separation property.

This work was supported by National Natural Science Foundation of China (21201062, 21172066), Hunan Provincial Natural Science Foundation of China (14JJ3113, 14JJ4045), Scientific Research Fund of Hunan Provincial Education Department (12C0115, 12C0116), and the Open Project Program of Key Laboratory of Theoretical Organic Chemistry and Function Molecule of Ministry of Education (Hunan University of Science and Technology, LKF1304).

Notes and references

- ‡ Crystal data for HNUST-4: C₇₅H₃₈N₆O₃₆Cu₆ (guest molecules removed with PLATON SQUEEZE¹²), M_r = 1980.41, Tetragonal, *I4-mmm*, *a* = *b* = 29.627(3) Å, *c* = 29.627 Å, $\alpha = \beta = \gamma = 90^\circ$, *V* = 26005(4) Å³, *Z* = 8, *D_c* = 1.012 g cm⁻³, *T* = 293(2) K, GOF = 1.199 based on *F*², final *R*₁ = 0.0958, *wR*₂ = 0.3059 [for 6539 data *I* > 2σ(*I*)]; CCDC: 1006012.
- (a) B. Xiao, P. S. Wheatley, X. Zhao, A. J. Fletcher, S. Fox, A. G. Rossi, I. L. Megson, S. Bordiga, L. Regli, K. M. Thomas, R. E. Morris, *J. Am. Chem. Soc.* 2007, **129**, 1203; (b) P. Nugent, Y. Belmabkhout, S. D. Burd, A. J. Cairns, R. Luebke, K. Forreest, T. Pham, S. Ma, B. Space, L. Wojtas, M. Eddaoudi, M. J. Zaworotko, *Nature*, 2013, **495**, 80.
 - (a) O. M. Yaghi, G. M. Li, H. L. Li, *Nature*, 1995, **378**, 703; (b) S. D. Burd, S. Ma, J. A. Perman, B. J. Sikora, R. Q. Snurr, P. K. Thallapally, J. Tian, L. Wojtas and M. J. Zaworotko, *J. Am. Chem. Soc.*, 2012, **134**, 3663.
 - U. Mueller, M. Schubert, F. Teich, H. Puetter, K. Schierle-Arndt, J. Pastre, *J. Mater. Chem.* 2006, **16**, 626.
 - (a) K. Koh, A. G. Wong-Foy and A. J. Matzger, *J. Am. Chem. Soc.*, 2009, **131**, 4184; (b) O. K. Farha, I. Eryazici, N. C. Jeong, B. G. Hauser, C. E. Wilmer, A. A. Sarjeant, R. Q. Snurr, S. T. Nguyen, A. Ö. Yazaydin, J. T. Hupp, *J. Am. Chem. Soc.* 2012, **134**, 15016; (c) H. Furukawa, N. Ko, Y. B. Go, N. Aratani, S. B. Choi, E. Choi, A. O. Yazaydin, R. Q. Snurr, M. O'Keefe, J. Kim, O. M. Yaghi, *Science*, 2010, **329**, 424; (d) O. K. Farha, A. özgür Yazayd, I. Eryazici, C. D. Malliakas, B. G. Hauser, M. G. Kanatzidis, S. T. Nguyen, R. Q. Snurr and J. T. Hupp, *Nat. Chem.* 2010, **2**, 944; (e) D. Q. Yuan, D. Zhao, D. F. Sun and H.-C. Zhou, *Angew. Chem., Int. Ed.*, 2010, **49**, 5357; (f) O. K. Farha, C. E. Wilmer, I. Eryazici, B. G. Hauser, P. A. Parilla, K. O'Neill, A. A. Sarjeant, S. T. Nguyen, R. Q. Snurr and J. T. Hupp, *J. Am. Chem. Soc.*, 2012, **134**, 9860.
 - (a) A. Fateeva, P. A. Chater, C. P. Ireland, A. A. Tahir, Y. Z. Khimyak, P. V. Wiper, J. R. Darwent, M. J. Rosseinsky, *Angew. Chem. Int. Ed. Engl.*, 2012, **51**, 7440; (b) D. Feng, W.-C. Chung, Z. Wei, Z.-Y. Gu, H.-L. Jiang, Y.-P. Chen, D. Darensbourg, H.-C. Zhou, *J. Am. Chem. Soc.*, 2013, **135**, 17105; (c) H.-L. Jiang, D. Feng, K. Wang, Z.-Y. Gu, Z. Wei, Y.-P. Chen, H.-C. Zhou, *J. Am. Chem. Soc.*, 2013, **135**, 13934; (d) J. J. Low, A. I. Benin, P. Jakubczak, J. F. Abrahamian, S. A. Faheem, R. R. Willis, *J. Am. Chem. Soc.*, 2009, **131**, 15834; (e) J. H. Cavka, S. Jakobsen, U. Olsbye, N. Guillou, C. Lamberti, S. Bordiga, K. P. Lillerud, *J. Am. Chem. Soc.* 2008, **130**, 13850; (f) J. Ehrenmann, S. K. Henninger, C. Janiak, *Eur. J. Inorg. Chem.* 2011, **2011**, 471; (g) G. Férey, C. Mellot-Draznieks, C. Serre, F. Millange, J. Dutour, S. Surblé, I. Margiolaki, *Science*, 2005, **309**, 2040.
 - (a) A. Demessence, D. M. D'Alessandro, M. L. Foo, J. R. Long, *J. Am. Chem. Soc.*, 2009, **131**, 8784; (b) S. S. Nagarkar, A. K. Chaudhari and S. K. Ghosh, *Inorg. Chem.*, 2012, **51**, 572; (c) H. J. Choi, M. Dincă, A. Dailly, J. R. Long, *Energy Environ. Sci.*, 2010, **3**, 117.

- 7 (a) H. Jasuja and K. S. Walton, *Dalton Trans.*, 2013, **42**, 15421; (b) J. Park, J.-R. Li, Y.-P. Chen, J. Yu, Z. U. Wang, L.-B. Sun, P. B. Balbuena, H.-C. Zhou, *Chem. Commun.*, 2012, **48**, 9995.
- 8 (a) H. Li, W. Shi, K. Zhao, H. Li, Y. Bing and P. Cheng, *Inorg. Chem.*, 2012, **51**, 9200; (b) S. J. Yang, J. Y. Choi, H. K. Chae, J. H. Cho, K. S. Nahm and C. R. Park, *Chem. Mater.*, 2009, **21**, 1893; (c) J. Chun, S. h Kang, N. Park, E. J. Park, X. Jin, K.-D. Kim, H. O. Seo, S. M. Lee, H. J. Kim, W. H. Kwon, Y.-K. Park, J. M. Kim, Y. D. Kim and S. U. Son, *J. Am. Chem. Soc.*, 2014, DOI: 10.1021/ja500362w.
- 10 9 (a) D. Ma, Y. Li, Z. Li, *Chem. Commun.*, 2011, **47**, 7377; (b) T. Wu, L. Shen, M. Luebbbers, C. Hu, Q. Chen, Z. Ni, R. I. Masel, *Chem. Commun.*, 2010, **46**, 6120; (c) J. Yang, A. Grzech, F. M. Mulder, T. J. Dingemans, *Chem. Commun.*, 2011, **47**, 5244; (d) J. M. Taylor, R. Vaidhyanathan, S. S. Iremonger and G. K. H. Shimizu, *J. Am. Chem. Soc.*, 2012, **134**, 14338; (e) T. A. Makal, X. Wang, H.-C. Zhou, *Cryst. Growth Des.*, **2013**, **13**, 4760.
- 10 (a) B. S. Zheng, J. F. Bai, J. G. Duan, L. Wojtas and M. J. Zaworotko, *J. Am. Chem. Soc.*, 2011, **133**, 748; (b) B. S. Zheng, Z. Yang, J. F. Bai, Y. Z. Li and S. H. Li, *Chem. Commun.*, 2012, **48**, 7025; (c) B. S. Zheng, H. T. Liu, Z. X. Wang, X. Y. Yu, P. G. Yi and J. F. Bai, *CrystEngComm*, 2013, **15**, 3517; (d) Z. X. Wang, B. S. Zheng, H. T. Liu, X. Lin, X. Y. Yu, P. G. Yi and R. R. Yu, *Cryst. Growth Des.*, 2013, **13**, 5001; (e) L. T. Du, S. L. Yang, L. Xu, H. H. Min and B. S. Zheng, *CrystEngComm*, 2014, **16**, 5520; (f) Z. Y. Lu, H. Xing, R. Sun, J. F. Bai, B. S. Zheng and Y. Z. Li, *Cryst. Growth Des.*, 2012, **12**, 1081; (g) J. G. Duan, Z. Yang, J. F. Bai, B. S. Zheng, Y. Z. Li and S. H. Li, *Chem. Commun.*, 2012, **48**, 3058.
- 25 (a) J. J. Perry IV, V. Ch. Kravtsov, G. J. McManus and M. J. Zaworotko, *J. Am. Chem. Soc.*, 2007, **129**, 10076; (b) X. F. Liu, M. Park, S. Hong, M. Oh, J. W. Yoon, J. S. Chang and M. S. Lah, *Inorg. Chem.*, 2009, **48**, 11507.
- 30 12 A. L. Spek, *J. Appl. Crystallogr.*, 2003, **36**, 7.
- 13 (a) S. Q. Ma, D. F. Sun, M. Ambrogio, J. A. Fillinger, S. Parkin, H. C. Zhou, *J. Am. Chem. Soc.*, 2007, **129**, 1858; (b) J. Y. Lee, J. Li, J. Jagiello, *J. Solid State Chem.* 2005, **178**, 2527.
- 35 14 (a) D. J. Collins and H.-C. Zhou, *J. Mater. Chem.*, 2007, **17**, 3154; (b) L. J. Murray, M. Dincă, J. R. Long, *Chem. Soc. Rev.*, 2009, **38**, 1294.
- 15 (a) T. K. Prasad, D. H. Hong, M. P. Suh, *Chem. Eur. J.* 2010, **16**, 14043; (b) P. Zhang, B. Li, Y. Zhao, X. Meng and T. Zhang, *Chem. Commun.*, 2011, **47**, 7722; (c) H. Hayashi, A. P. Cote, H. Furukawa, M. O'Keeffe, O. M. Yaghi, *Nat. Mater.*, 2007, **5**, 501; (b) A. Phan, C. J. Doonan, F. J. Uribe-Romo, C. B. Knobler, M. O'Keeffe, O. M. Yaghi, *Acc. Chem. Res.*, 2010, **43**, 58.
- 40 16 J.-R. Li, Y. Ma, M. C. McCarthy, J. Sculley, J. Yu, H.-K. Jeong, P. B. Balbuena and H.-C. Zhou, *Coord. Chem. Rev.*, 2011, **255**, 1791.
- 45